S.P. REPETSKY,[1] O.V. TRETIAK,[2] I.G. VYSHIVANAYA [2]

[1] Taras Shevchenko National University of Kyiv
(64, Volodymyrs'ka Str., Kyiv 01601, Ukraine; e-mail: srepetsky@univ.kiev.ua)
[2] Taras Shevchenko National University of Kyiv, Institute of High Technologies
(4g, Academician Glushkov Ave., Kyiv 03127, Ukraine)

PACS 73.20.At

ELECTRON STRUCTURE
AND ELECTRIC CONDUCTIVITY
OF GRAPHENE WITH A NITROGEN IMPURITY

On the basis of the tight-binding model with the use of exchange-correlation potentials, the electron structure and the electric conductivity of graphene with a nitrogen impurity have been studied in the framework of density functional theory. The wave functions of $2s$ and $2p$ states of neutral noninteracting carbon atoms are selected as the basis ones. Band hybridization was found to result in the splitting of the electron energy spectrum near the Fermi level. In the nitrogen-doped graphene, owing to the overlapping of $2p$ energy bands, the mentioned gap is realized as a quasi-gap, in which the electron density of states has a much lower value in comparison with the other spectral region. It is found that an increase in the nitrogen concentration reduces the electric conductivity of graphene, although the density of states at the Fermi level grows at that. Hence, the reduction of the electric conductivity is associated with a sharper decrease in the relaxation time for electron states.

K e y w o r d s: nitrogen-doped graphene, electron energy spectrum, tight-binding model, electric conductivity

One of the ways to intentionally modify the graphene properties in order to use them in nano- and spin-electronics consists in doping graphene with atoms of other elements. Impurities can stimulate a change of the crystal lattice symmetry and the formation of additional energy gaps with the width depending on the impurity type and the concentration [1–7].

In works [1, 2], the gapping of the electron energy spectrum near the Dirac point, when the impurity concentration increases, was studied analytically in the framework of the simple Lifshitz single-band model for a disordered crystal. In work [3], the electron structure in an isolated graphene monolayer, as well as in bilayered and three-layer graphene grown on ultrathin layers of hexagonal boron nitride, h-BN, was considered in the framework of density functional theory with the use of the method of pseudopotential. It was shown that, in the case of a single graphene layer on an h-BN monolayer, there emerges an energy gap 57 meV in width. In work [4], an analogous method was used to study graphene with aluminum, silicon, phosphorus, and sulfur impurities. It was shown that

graphene doped with the phosphorus impurity to 3% has a 0.67-eV gap.

In work [5], the electron structure of graphene was studied in the framework of density functional theory with the use of a generalized gradient approximation for the exchange-correlation potential. With the help of the software package QUANTUM-ESPRESSO, a possibility of gapping in the energy spectrum of graphene doped with boron and nitrogen atoms (a gap width of 0.49 eV), as well as boron atoms and lithium ones adsorbed on the surface (a gap width of 0.166 eV), was demonstrated.

In works [6, 7], methods that allow a direct measurement of the Dirac point and Fermi energies in graphene included in various heterostructures were proposed and applied. In particular, in the case of graphene in a multilayered Al_2O_3/graphene/SiO_2/Si structure, the energy of Dirac point was found to equal 3.58 eV, and the Fermi energy to 3.25 eV [6].

However, the influence of impurities on the electron structure and the related properties of graphene has not been studied enough. In this work, on the basis of the multiband model of tight binding, we considered the influence of the nitrogen impurity on the electron structure and the electric conductivity of graphene.

The researches were carried out, by using the method of cluster expansion of two-time Green's functions for the electron subsystem in a disordered crystal, which was developed in works [8–13]. In this method, the approximation of coherent potential comprises the zeroth-order approximation. The contributions of the processes of electron scattering by clusters were shown to decrease as a certain small parameter, when the number of sites in the clusters increases [8]. In the cited works, the electron-electron and electron-phonon interactions were described on the basis of a diagram technique for temperature Green's functions. The method is a generalization of the known technique for a uniform electron gas [14], with the known relations between the spectral representations for the temperature and two-time Green's functions being used at that.

While calculating the energy spectrum and the electric conductivity of nitrogen-doped graphene, the actual wave functions of the $2s$ and $2p$ states of neutral noninteracting carbon atoms are chosen to form the basis set. The wave functions of neutral non-interacting atoms are determined from the Cohn–Sham equation of density functional theory. The exchange-correlation potential is calculated in the meta-generalized gradient approximation [15]. The matrix elements of the Hamiltonian are calculated, by using the Slater–Koster method [16], and only first three coordination spheres are taken into account.

Neglecting the contributions from the electron scattering by clusters containing three and more atoms (they are small in the parameter indicated above [8]), we obtain the expression for the electron density of states,

$$g(\varepsilon) = \frac{1}{\nu} \sum_{i,\gamma,\sigma,\lambda} P_{0i}^{\lambda} g_{0i\gamma\sigma}^{\lambda}(\varepsilon),$$

$$g_{0i\gamma\sigma}^{\lambda}(\varepsilon) = -\frac{1}{\pi}\mathrm{Im}\Big\{ \widetilde{G} + \widetilde{G}\, t_{0i}^{\lambda}\, \widetilde{G} + \sum_{\substack{(nj)\neq(0i) \\ \lambda'}} P_{nj0i}^{\lambda'/\lambda} \times$$

$$\times \widetilde{G} \left[t_{nj}^{\lambda'} + T^{(2)\lambda 0_i,\lambda n_j} + T^{(2)\lambda' n_j,\lambda 0_i} \right] \widetilde{G} \Big\}^{0_i\gamma\sigma,0_i\gamma\sigma},$$

(1)

where i is the sublattice number, ν the number of sublattices, γ the energy band number, and σ the quantum number describing the electron spin projection on the axis z. In Eq. (1),

$$T^{(2)n_1 i_1,n_2 i_2} = \left[I - t^{n_1 i_1}\, \widetilde{G}\, t^{n_2 i_2}\, \widetilde{G} \right] \times$$

$$\times t^{n_1 i_1}\, \widetilde{G}\, t^{n_2 i_2} \left[I + \widetilde{G}\, t^{n_1 i_1} \right],$$
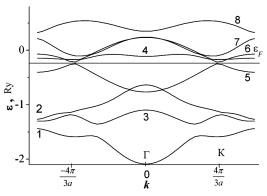
where $t^{n_1 i_1}$ is the operator of scattering by one site,

$$t^{n_1 i_1} = \left[I - \left(\Sigma^{n_1 i_1} - \sigma^{n_1 i_1} \right) \widetilde{G} \right] \left(\Sigma^{n_1 i_1} - \sigma^{n_1 i_1} \right), \quad (2)$$
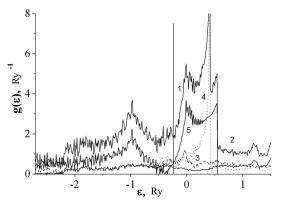
and P_{0i}^{λ} and $P_{nj\,0i}^{\lambda'/\lambda}$ are the probability and the conditional probability, respectively, for the arrangement of the atoms of sort λ. In expressions (1) and (2), $\tilde{G} = \tilde{G}_r$ is retarded Green's function of the effective medium described by the coherent potential $\sigma^{n_1 i_1}$.

Using the Kubo formula and the indicated diagram technique, in works [9–12], an expression for the electric conductivity of the electron subsystem in a disordered crystal was obtained. Neglecting the contributions of the scattering by clusters composed of two and more sites, the static conductivity can be written in the form [11–13]
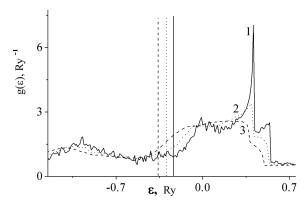
$$\sigma_{\alpha\beta} = \frac{e^2 \hbar}{4\pi V_1} \Bigg\{ \int_{-\infty}^{\infty} d\varepsilon_1 \frac{\partial f}{\partial \varepsilon_1} \sum_{s,s'=+,-} (2\delta_{ss'} - 1) \times$$

$$\times \sum_{\sigma\gamma,i} \Big\{ \left[\nu_\beta\, \widetilde{K} \left(\varepsilon_1^{s'}, \nu_\alpha, \varepsilon_1^{s'} \right) \right] +$$

$$+ \sum_{\lambda,m_{\lambda i}} P_{0i}^{\lambda m_{\lambda i}}\, \widetilde{K} \left(\varepsilon_1^{s'}, \nu_\beta, \varepsilon_1^{s} \right) t_{0i}^{\lambda m_{\lambda i}} (\varepsilon_1^{s}) \times$$

$$\times \widetilde{K} (\varepsilon_1^{s}, \nu_\alpha, \varepsilon_1^{s'}) t_{0i}^{\lambda m_{\lambda i}} (\varepsilon_1^{s'}) + \sum_{\lambda,m_{\lambda i}} P_{0i}^{\lambda m_{\lambda i}} \times$$

$$\times \sum_{\substack{lj \neq 0i \\ \lambda', m_{\lambda' j}}} P_{lj0i}^{\lambda' m_{\lambda' j}/\lambda m_{\lambda i}} \left[\left[\widetilde{K} \left(\varepsilon_1^{s'}, \nu_\beta, \varepsilon_1^{s} \right) \nu_\alpha\, \widetilde{G} \left(\varepsilon_1^{s'} \right) \right] \times$$

$$\times T^{(2)\lambda m_{\lambda i}0i,\lambda' m_{\lambda' j}lj} (\varepsilon_1^{s'}) +$$

$$+ \left[\widetilde{K} \left(\varepsilon_1^{s'}, \nu_\beta, \varepsilon_1^{s} \right) \nu_\alpha\, \widetilde{G} \left(\varepsilon_1^{s'} \right) \right] \times$$

$$\times T^{(2)\lambda' m_{\lambda' j}lj,\lambda m_{\lambda i}0i} (\varepsilon_1^{s'}) +$$

$$+ \left[\widetilde{K} \left(\varepsilon_1^{s}, \nu_\alpha, \varepsilon_1^{s'} \right) \nu_\beta\, \widetilde{G} \left(\varepsilon_1^{s} \right) \right] \times$$

$$\times T^{(2)\lambda m_{\lambda i}0i,\lambda' m_{\lambda' j}lj} (\varepsilon_1^{s}) +$$

$$+ \left[\widetilde{K} \left(\varepsilon_1^{s}, \nu_\alpha, \varepsilon_1^{s'} \right) \nu_\beta\, \widetilde{G} \left(\varepsilon_1^{s} \right) \right] \times$$

$$\times T^{(2)\lambda' m_{\lambda' j}lj,\lambda m_{\lambda i}0i} (\varepsilon_1^{s}) + \widetilde{K} \left(\varepsilon_1^{s'}, \nu_\beta, \varepsilon_1^{s} \right) \times$$

$$\times \left(t_{lj}^{\lambda' m_{\lambda' j}} (\varepsilon_1^{s})\, \widetilde{K} \left(\varepsilon_1^{s}, \nu_\alpha, \varepsilon_1^{s'} \right) t_{0i}^{\lambda m_{\lambda i}} (\varepsilon_1^{s'}) +$$

$$+ t_{lj}^{\lambda' m_{\lambda' j}} (\varepsilon_1^{s})\, \widetilde{K} \left(\varepsilon_1^{s}, \nu_\alpha, \varepsilon_1^{s'} \right) T^{(2)\lambda m_{\lambda i}0i,\lambda' m_{\lambda' j}lj} \left(\varepsilon_1^{s'} \right) +$$

Fig. 1. Dependences of the electron energy in pure graphene on the absolute value of wave vector **k** for the energy bands $2s$ (*1* and *2*), $2p_x$ (*3* and *4*), $2p_z$ (*5* and *6*), and $2p_y$ (*7* and *8*)

Fig. 2. Energy dependence of the electron density of states, $g(\varepsilon)$, in graphene doped with the nitrogen impurity to 1%: total density of states (*1*), partial density of states $2s$ (*2*), $2p_x$ (*3*), $2p_y$ (*4*), and $2p_z$ (*5*)

Fig. 3. Energy dependences of the electron density of states, $g(\varepsilon)$, in graphene doped with the nitrogen impurity to 1 (*1*), 5 (*2*), and 10% (*3*)

$$+ T^{(2)\lambda' m_{\lambda' j} lj, \lambda m_{\lambda i} 0i} \left(\varepsilon_1^s\right) \widetilde{K}\left(\varepsilon_1^s, \nu_\alpha, \varepsilon_1^{s'}\right) t_{0i}^{\lambda m_{\lambda i}}\left(\varepsilon_1^{s'}\right) +$$

$$+ T^{(2)\lambda' m_{\lambda' j} lj, \lambda m_{\lambda i} 0i}\left(\varepsilon_1^s\right) \widetilde{K}\left(\varepsilon_1^s, \nu_\alpha, \varepsilon_1^{s'}\right) \times$$

$$\times T^{(2)\lambda m_{\lambda i} 0i, \lambda' m_{\lambda' j} lj}\left(\varepsilon_1^{s'}\right) + T^{(2)\lambda' m_{\lambda' j} lj, \lambda m_{\lambda i} 0i}\left(\varepsilon_1^{s'}\right) \times$$

$$\times \widetilde{K}\left(\varepsilon_1^s, \nu_\alpha, \varepsilon_1^{s'}\right) T^{(2)\lambda' m_{\lambda' j} lj, \lambda m_{\lambda i} 0i}\left(\varepsilon_1^{s'}\right)\Big)\Big]\Big\}^{0i\gamma\sigma, 0i\gamma\sigma} +$$

$$+ \int\limits_{-\infty}^{\infty}\int\limits_{-\infty}^{\infty} d\varepsilon_1 d\varepsilon_2 f(\varepsilon_1) f(\varepsilon_2) \left\langle \triangle\, G_{\alpha\beta}^{II}(\varepsilon_1, \varepsilon_2)\right\rangle\Bigg\}, \qquad (3)$$

where $\widetilde{K}\left(\varepsilon_1^s, \nu_\alpha, \varepsilon_1^{s'}\right) = \widetilde{G}\left(\varepsilon_1^{s'}\right)\nu_\alpha\,\widetilde{G}\left(\varepsilon_1^{s'}\right),$

$\widetilde{G}\left(\varepsilon_1^+\right) = \widetilde{G}_r\left(\varepsilon_1\right)\,\widetilde{G}_r\left(\varepsilon_1^-\right) = \widetilde{G}_a\left(\varepsilon_1\right) = \left(\widetilde{G}_r\left(\varepsilon_1\right)\right)^*,$

$f(\varepsilon)$ is the Fermi distribution function, V the volume of the elementary cell, e the electron charge, and $\hbar$ Planck's constant. In formula (3), $\triangle G_{\alpha\beta}^{II}(\varepsilon_1, \varepsilon_2)$ is a component of two-particle Green's function, which is expressed in terms of the vertex function for the mass operator of electron-electron interaction [11]. Numerical calculations showed that the contribution of the last term does not exceed a few percent; therefore, it was neglected in our further calculations. The operator ν_α of the α-projection of the electron velocity in formula (3) equals

$$\nu_{\alpha i, i'}(\mathbf{k}) = \frac{1}{\hbar}\frac{\partial h_{i,i'}(\mathbf{k})}{\partial \mathbf{k}_\alpha}.$$

The energy spectrum and the electric conductivity of graphene are calculated for the temperature $T = 0$ K. In Fig. 1, the dependences of the electron energy ε in pure graphene on the wave vector **k** obtained from the condition for Green's function poles are shown. The vector **k** is assumed to be directed from the center of the Brillouin zone (point Γ) to the Dirac point (point K). In Fig. 1, $a = \sqrt{3}a_0$, where $a_0 = 0.142$ nm is the minimum distance between carbon atoms.

In Figs. 2 and 3, the energy dependences of the electron density of states, $g(\varepsilon)$, in nitrogen-doped graphene, which were calculated by formula (1), are depicted. Nitrogen atoms replace carbon ones at the sites of the graphene crystal lattice. The vertical lines mark the corresponding positions of the Fermi level. In Fig. 3, a section of the energy spectrum near the Fermi level is exhibited.

From Figs. 1 to 3, it is evident that the band hybridization results in the gapping in the $2p_z$ energy band, which is connected with the $(pp\pi)$-bond [16]. Electron states in that band are described by atomic wave functions of the z-symmetry. Carbon atoms in pure graphene are located in two nonequivalent positions of the elementary cell. As a result, two energy bands correspond to the same bond type (Fig. 1). The Fermi level is located in the middle of the gap. Its position corresponds to the position of the Dirac point. The gap width equals $0.008\,\mathrm{Ry} \approx 1\,\mathrm{eV}$, and the Fermi level $\varepsilon_{\mathrm{F}} = -0.23\,\mathrm{Ry} \approx -3.13\,\mathrm{eV}$. In graphene with the nitrogen impurity, owing to the overlapping of $2p$ bands, the gap mentioned above manifests itself as a quasi-gap in the electron energy spectrum. The electron density of states in a vicinity of this quasi-gap is much lower in comparison with the neighbor spectral regions (Fig. 2). The position of the Fermi level in the energy spectrum depends on the nitrogen concentration and falls within the energy interval $-0.36\,\mathrm{Ry} \leq \varepsilon_{\mathrm{F}} \leq -0.23\,\mathrm{Ry}$. As the nitrogen concentration increases, the quasi-gap width decreases, and the Fermi level shifts toward the left quasi-gap edge. The theoretical values of Fermi level energy for pure graphene agree with experimental values for graphene in the multilayered $\mathrm{Al_2O_3/graphene/SiO_2/Si}$ structure [6].

In Fig. 4, the dependences of the components $\sigma_{\alpha\beta}$ of the static electric conductivity tensor on the nitrogen impurity concentration calculated by formula (3) for the temperature $T = 0\,\mathrm{K}$ are shown. The x-axis is directed toward the nearest neighbor atom. The conductivity was calculated for nitrogen concentrations denoted by points, and the points are connected by straight lines. As is seen from Fig. 4, the conductivity of graphene decreases, as the nitrogen concentration grows. For comparison, the experimental value of electric conductivity in graphite at the temperature $T = 300\,\mathrm{K}$ equals $\sigma = 9.82 \times 10^5\,\Omega^{-1}\mathrm{m}^{-1}$ [17].

In Fig. 5, the concentration dependences of the partial $2s$ and $2p$ components of the σ_{xx} component of the static electric conductivity tensor are shown. One can see that the main contribution to the conductivity is made by the electron states that are described by the $2p_z$ atomic wave functions [16].

In order to examine the nature of the concentration dependence of the electric conductivity in graphene, let us write down the limiting expression for this parameter in the case of weak scattering, which follows
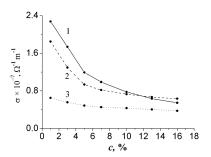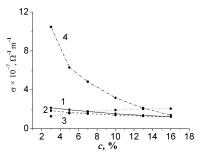

Fig. 4. Dependences of the components of the electric conductivity tensor on the nitrogen impurity concentration c: σ_{xx} (*1*), σ_{yy} (*2*), and σ_{xy} (*3*)
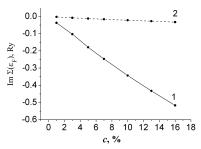

Fig. 5. Dependences of the partial $2s$ and $2p$ components of the component σ_{xx} of the electric conductivity tensor on the nitrogen impurity concentration c: $2s$ (*1*), $2p_x$ (*2*), $2p_y$ (*3*), and $2p_z$ (*4*)

from the general formula (3) in the single-band approximation [12]:

$$\sigma_{\alpha\alpha} = \frac{e^2 \hbar g(\varepsilon_{\mathrm{F}}) \nu^2(\varepsilon_{\mathrm{F}})}{3\Omega_1 \mid \Sigma''(\varepsilon_{\mathrm{F}}) \mid},$$

where $\Sigma''(\varepsilon_{\mathrm{F}}) = \mathrm{Im}\Sigma(\varepsilon_{\mathrm{F}})$ is the imaginary part of the mass operator of Green's function, $\nu(\varepsilon_{\mathrm{F}})$ the electron velocity at the Fermi level, and Ω_1 the volume per one atom. The relaxation time of electron states, $\tau(\varepsilon_{\mathrm{F}})$, is determined by the relation $|\Sigma''(\varepsilon_{\mathrm{F}})| \, \tau(\varepsilon_{\mathrm{F}}) = \hbar$.

In Fig. 6, the concentration dependences of the total imaginary part of the mass operator of Green's function and its partial $2p_z$ component are shown. In Fig. 7, the concentration dependences of the total electron density of states at the Fermi level and its partial $2p_z$ component are exhibited. Since the electron density of states at the Fermi level grows with the nitrogen concentration (Fig. 7), the reduction of the electric conductivity (Figs. 4 and 5) is explained by a more drastic reduction of the relaxation time for electron states (Fig. 6).

Fig. 6. Dependences of the (*1*) total imaginary part of the mass operator of Green's function for graphene and (*2*) its partial $2p_z$ component on the nitrogen impurity concentration c
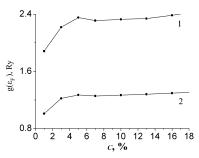

Fig. 7. Dependences of the (*1*) total electron density of states in graphene at the Fermi level and (*2*) its partial $2p_z$ component on the nitrogen impurity concentration c

Thus, it is found that the band hybridization results in the splitting of the electron energy spectrum near the Fermi level. The gap width equals 0.008 Ry ≈ 1 eV, and the Fermi level $\varepsilon_{\rm F} = -0.23$ Ry ≈ -3.13 eV. In graphene doped with the nitrogen impurity, owing to the overlapping of p bands, the indicated gap manifests itself as a quasi-gap. The position of the Fermi level in the energy spectrum depends on the nitrogen concentration and falls within the energy interval -0.36 Ry $\leq \varepsilon_{\rm F} \leq -0.23$ Ry. As the nitrogen concentration increases, the quasi-gap width decreases, and the Fermi level shifts toward the left quasi-gap edge. The reduction of the graphene conductivity at higher nitrogen concentrations is connected with a decrease of the relaxation time of electron states.

1. Yu.V. Skrypnyk and V.M. Loktev, Phys. Rev. B **73**, 241402 (2006).
2. Yu.V. Skrypnyk and V.M. Loktev, Phys. Rev. B **75**, 245401 (2007).
3. C. Yelgel and G.P. Srivastava, Appl. Surf. Sci. **258**, 8338 (2012).
4. D.A. Pablo, Chem. Phys. Lett. **492**, 251 (2010).
5. D. Xiaohui, W. Yanqun, D. Jiayu, K. Dongdong, and Z. Dengyu, Phys. Lett. A **365**, 3890 (2011).
6. K. Xu, C. Zeng, Q. Zhang, R. Yan, P. Ye, K. Wang, A.C. Seabaugh, H.G. Xing, J.S. Suehle, C.A. Richter, D.J. Gundlach, and N.V. Nguyen, Nano Lett., **13**, 131 (2013).
7. S. Kim, I. Jo, D.C. Dillen, D.A. Ferrer, B. Fallahazad, Z. Yao, S.K. Banerjee, and E. Tutuc, Phys. Rev. Lett. **108**, 116404 (2012).
8. S.P. Repetsky and T.D. Shatnyi, Teor. Mat. Fiz. **131**, 456 (2002).
9. S.P. Repetsky and I.G. Vyshyvanaya, Metallofiz. Noveish. Tekhnol. **26**, 887 (2004).
10. S.P. Repetskii and I.G. Vyshyvanaya, Phys. Met. Metallogr. **99**, 558 (2005).
11. S.P. Repetsky and I.G. Vyshyvanaya, Metallofiz. Noveish. Tekhnol. **29**, 587 (2007).
12. S.P. Repetsky, I.G. Vyshyvanaya, V.V. Shastun, and A.F. Mel'nik, Metallofiz. Noveish. Tekhnol. **33**, 425 (2011).
13. S.P. Repetsky, O.V. Tretyak, I.G. Vyshyvanaya, and V.V. Shastun, Ukr. J. Phys. **13**, 189 (2012).
14. A.A. Abrikosov, L.P. Gor'kov, and I.E. Dzyaloshinskij, *Methods of Quantum Field Theory in Statistical Physics* (Prentice Hall, Englewood Cliffs, NJ, 1963).
15. J. Sun, M. Marsman, G.I. Csonka, A. Ruzsinszky, P. Hao, Y. Kim, G. Kresse, and J.P. Perdew, Phys. Rev. B **84**, 035117 (2011).
16. J.C. Slater and G.F. Koster, Phys. Rev. **94**, 1498 (1954).
17. A.R. Ubbelohde and F.A. Lewis, *Graphite and Its Crystal Compounds* (Clarendon Press, London, 1960).

С.П. Репецький, О.В. Третяк, І.Г. Вишивана

ЕЛЕКТРОННА
СТРУКТУРА ТА ЕЛЕКТРОПРОВІДНІСТЬ
ГРАФЕНУ З ДОМІШКОЮ АЗОТУ

Р е з ю м е

На основі моделі сильного зв'язку з використанням обмінно-кореляційних потенціалів у теорії функціонала густини досліджена електронна структура та електропровідність графену з домішкою азоту. В ролі базису вибираються хвильові функції 2*s*-, 2*p*-станів нейтральних невзаємодіючих атомів вуглецю. Встановлено, що гібридизація зон призводить до розщеплення енергетичного спектра електронів в області рівня Фермі. У графені з домішкою азоту завдяки перекриттю 2*p*-енергетичних зон згадана вище щілина проявляється як квазіщілина, в області якої густина електронних станів має значно менше значення порівняно з іншою областю спектра. Встановлено, що зі збільшенням концентрації азоту електропровідність графену зменшується. Оскільки зі збільшенням концентрації азоту густина станів на рівні Фермі зростає, то зменшення електропровідності зумовлено більш різким зменшенням часу релаксації електронних станів.